An analysis of Coriolis mass flow chips with a bypass

B.N.A Sikkens

6/25/2013
Bachelor thesis
Bachelor Advanced Technology
Transducers Science and Technology Group
Faculty of Electrical Engineering, Mathematics and Computer Science

Bachelor assignment committee:

R.J Wiegerink **Chairman**

J. Groenesteijn **Supervisor**

A. de Boer **External member**

Abstract
In this report a study is done on the behavior of a Coriolis mass flow sensor chip with bypass tubes. The goal of this report is to obtain a model that can predict the ratio of the bypass flow compared to the Coriolis sensor tube flow. For verification this model is tested by measuring said Coriolis mass flow sensor chips and comparing these measurements to the model. This is at the same time also a test report for these chips. Furthermore an analysis is done on how to improve the predicted behavior. An overview of the measurement set-up is presented and the background of the workings behind a Coriolis mass flow sensor chip. The outcome of this research is that the model can give a reasonable prediction on flows, but is not entirely verified yet.

Table of Contents

1 Introduction

This Bachelor's assignment report is about the theoretical analysis and the experiments with the new-designed Coriolis mass-flow sensor chips equipped with a bypass flow tube. In this introduction, some background information is given about the project which involves the sensor chips. Then the research objectives will be identified, which are finally collected into the structure of this report.

1.1 PRECISE

One of the goals of the PRECISE project is to develop a MEMS-based monopropellant micro Chemical Propulsion System (µCPS) for highly accurate attitude control of satellites[precise].
ESA sees µCPS as a revolutionary way to be used for electrical and chemical propulsion, since it is highly integrated, lightweight and consumes little power. One of the big advantages of these systems is that the entire thruster, with its many modules, can be produced on a silicon wafer with a small size and weight. Project PRECISE strives to bring the many competences of companies, institutes and universities together for the R&D of this system for market demands

This project is a collaboration between several companies and universities with the University of Twente being one of the 2 universities. The Transducers Science and Technology group within the University of Twente participates in this project and will deliver some components for the actual micro thruster and the test facility diagnostics for the micro thruster, of which the Coriolis mass flow sensor is one.

1.2 The bachelor assignment

This bachelor assignment will be focused on one of the test facility diagnostics for the micro thruster, being a Coriolis mass flow sensor chip, which can measure the mass flow, in this case the fuel, through a tube. Although mass flow sensors have been available on the market for some time the sensors that are on the market are only suitable for very large flows and not for the small flows that are used for example in the PRECISE project. Although the Coriolis mass flow sensor is better for usage in this application, the sensitivity is too high and therefore bypass tubes are added to make the sensor suitable for use in the PRECISE project. The objectives of this bachelor project with respect to this chip are:

- A theoretical analysis of the flows through the chip and the bypass to give a prediction if the flow through the Coriolis mass flow sensor chip is a measure of the entire flow. In other words: What is the ratio between these flows and how does this ratio behave for different parameters?
- A test of the chips with water to check the validity of the theoretical analysis

This bachelor assignment has several goals:

- To obtain a model able to describe the flow ratios and flows within a Coriolis mass flow sensor chip, with as input design parameters:
    - Fluid parameters
    - Tube dimensions
- To obtain the measurement range of the designed chips by measuring its input flow and Coriolis flow in order to determine the ratio
- To obtain insight in ways to improve the desired chip behavior

1.3 Outline of the report

Chapter 2 consists of the background of the new Coriolis mass flow chips. Chapter 3 focuses on the analysis of the flows in the bypass tubes and the Coriolis sensor tubes. Chapter 4 makes an analysis on the properties of the chips that will be measured. Chapter 5 tells about the measurement set-up of the experiments. Chapter 6 lists the results of these experiments, while these will be discussed in chapter 7. And finally the conclusions of this research together with my recommendations are listed in chapter 8.

2 Coriolis chips

To analyze the behavior of a Coriolis mass flow sensor with bypass tubes one needs to have knowledge of a Coriolis mass flow sensor without bypass tubes.

2.1 The fundamental principle of operation

A Coriolis type flow sensor is made up by a vibrating tube. If you have a fluid flow inside this tube and you actuate this tube such that it vibrates with a certain frequency, then because of this vibration the moving mass of this flow changes its velocity. The adaptation in velocity gives a force, the so-called Coriolis force, which adds another type of movement to the tube. This movement is dependent on the mass flow, the actuation frequency of the external vibration and the length of the tube with the following formula:

$$F_c = -2 \cdot L_y \cdot (\omega_{am} \cdot \varphi_m)$$

In this formula L_y is the length of the tube in meters, ω_{am} being the frequency of the torsional mode in rad/s and φ_m the mass flow in kg/s.

The external vibration is applied through the Lorentz force, an AC current is applied through a wire on top of the tube while the tube is positioned in a static magnetic field. Because of the AC-current the Lorentz force constantly changes direction, resulting in a vibrating tube.

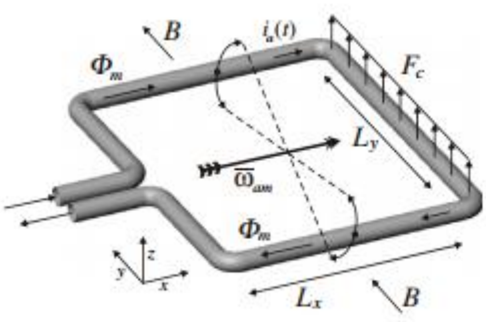

Figure 1: Schematic depiction of the Coriolis flow sensor tube[TST]

2.2 Modeling of the sensor

The sensor depicted in figure 1 has two vibration modes: the detection mode induced by the Coriolis force corresponding to rotation around the y-axis and the torsional actuation mode indicated by ω_{am}which boils down to a rotation around the x-axis. The angular rotations of both modes can be described by the following differential equation:

$$J_m \cdot \frac{d^2\theta_m(t)}{dt^2} + \gamma_m \cdot \frac{d\theta_m(t)}{dt} + K_m \cdot \theta_m(t) = T_m(t)$$

The subscripts correspond to the different modes. J is the moment of inertia in NM s^{-2}, θ is the phase of the modes in degrees, K is the spring constant in Nm, γ is the damping constant in Nm/s and T is the torque of the mode in N*m. Next we can express the actuation current as:

$$i_a(t) = I_a \cdot \cos(\omega_a \cdot t)$$

With I being the current in amperes. This AC-current together with the external magnetic field B makes the following actuation torque:

$$T_a(t) = L_x \cdot L_y \cdot B \cdot I_a \cdot \cos(\omega_a \cdot t)$$

If the differential equation is solved for the quasi-static case, which is valid when the actuation frequency is low, the following result can be obtained:

$$\theta_a(t) = \frac{T_a(t)}{K_a} = \frac{L_x \cdot L_y \cdot B}{K_a} \cdot I_a \cdot \cos(\omega_a \cdot t)$$

Usually the system is driven at resonance frequency so that the transfer is multiplied by the quality factor, while the phase is -90 degrees with respect to the current:

$$\theta_{ar}(t) = \frac{T_a(t)}{K_a} = \frac{L_x \cdot L_y \cdot B \cdot Q_a}{K_a} \cdot I_a \cdot \cos\left(\omega_{ar} \cdot t - \frac{1}{2} \cdot \pi\right)$$

To obtain the angular velocity of the vibration this phase has to be differentiated with respect to time:

$$\omega_{am}(t) = \frac{d\theta_{ar}(t)}{dt} = \frac{L_x \cdot L_y \cdot B \cdot \omega_{ar} \cdot Q_a}{K_a} \cdot I_a \cdot \cos(\omega_{ar} \cdot t)$$

The Coriolis force F_c is as stated before a product between the angular velocity and the mass flow. Therefore if you look at figure 1 there will only be a force on the segments in the y-direction. The segment indicated by F_c experiences the most Coriolis force and generates a Torque:

$$T_d(t) = -2 \cdot L_x \cdot L_y \cdot \varphi_m \cdot \omega_{am}(t) = \frac{{L_x}^2 \cdot {L_y}^2 \cdot B \cdot \omega_{ar} \cdot Q_a}{K_a} \cdot I_a \cdot \varphi_m \cdot \cos(\omega_{ar} \cdot t)$$

This torque will excite a mode with frequency ω_{dr} which has its own equation. There are 2 situations which can happen: one where the detection frequency is higher than the actuation frequency and a situation where the actuation frequency is higher than the detection frequency. In the situation where the actuation frequency is higher than the detection frequency there is a phase shift of 180 degrees of the detection signal with respect to the actuation signal. For the situation where the actuation frequency is higher the amplitude is lowered by a factor $\left(\frac{\omega_{dr}}{\omega_{ar}}\right)^2$ The resulting detection angle is then given by:

$$\theta_d(t) = \left(\frac{\omega_{dr}}{\omega_{ar}}\right)^2 \cdot \frac{T_d(t)}{K_d} = \left(\frac{\omega_{dr}}{\omega_{ar}}\right)^2 \cdot \frac{{L_x}^2 \cdot {L_y}^2 \cdot B \cdot \omega_{ar} \cdot Q_a}{K_a \cdot K_d} \cdot I_a \cdot \varphi_m \cdot \cos(\omega_{ar} \cdot t)$$

When this formula is viewed together with the formula of the actuation angle it can be clearly seen that the angles are 90 degrees out of phase, while the amplitudes have the following ratio:

$$\frac{\theta_d(t)}{\theta_a(t)} = 2 \cdot \left(\frac{\omega_{dr}}{\omega_{ar}}\right)^2 \cdot \frac{L_x \cdot L_y}{K_d} \cdot \omega_{ar} \cdot \varphi_m$$

If the detection frequency is higher than the actuation frequency then the angle is just proportional to the torque:

$$\theta_d(t) = \frac{T_d(t)}{K_d} = 2\frac{{L_x}^2 \cdot {L_y}^2 \cdot B \cdot \omega_{ar} \cdot Q_a}{K_a \cdot K_d} \cdot I_a \cdot \varphi_m \cdot \cos\left(\omega_{ar} \cdot t\right)$$

Again the detection angle and the actuation angle are 90 degrees out of phase with respect to each other. The ratio of the amplitudes is now:

$$\frac{\theta_d(t)}{\theta_a(t)} = 2 \cdot \frac{L_x \cdot L_y}{K_d} \cdot \omega_{ar} \cdot \varphi_m$$

What can be seen from the formulas is that the modes of operation are very similar; the only difference is a frequency ratio.[TST]

2.3 Flow measurement

The Coriolis force that acts on the tube has to be measured and this is done through the use of counter phase measurement; there are two comb –shaped readout capacitors that are each fed with signals that are 180 degrees out of phase with respect to each other. The signals measured by each capacitor set each are subtracted from each other and the difference in phases of the signals is a measure for the mass flow. The electronic set in total is depicted in figure 2

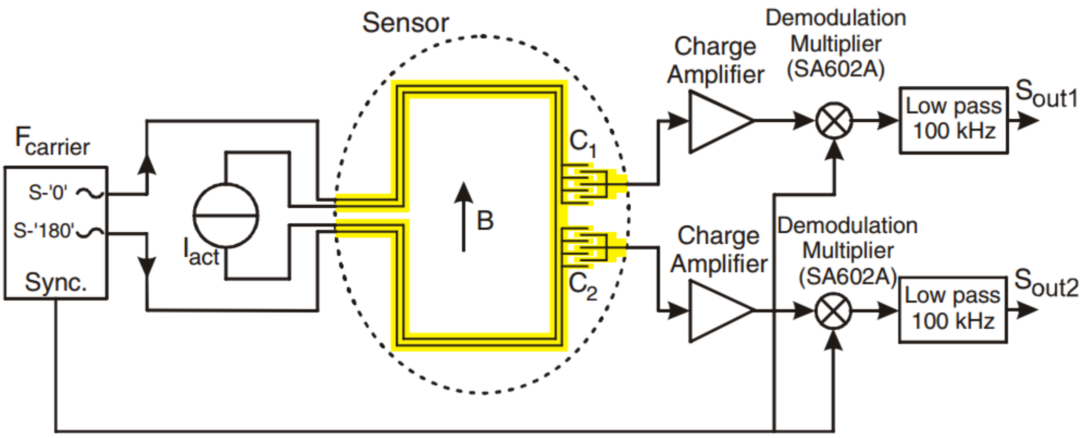

Figure 2: Schematic diagram of the actuation and readout electronics [TST]

3 Flow modeling

3.1 Fluid model

To model the behaviour of the mass flows the basics of fluid dynamics are used.

The first laws that are used are Bernouilli's law and Poisseuille's equation for the flows inside tubes:

$$p_{ext} = p_{i,in} + \frac{1}{2}\rho \cdot {v_i}^2$$

$$Q_i = \frac{\pi \cdot {d_i}^2 \cdot (p_{i,in} - p_{i,out})}{128 \cdot \mu \cdot l_i}$$

Where the first one describes the pressure you apply on a certain fluid within a tube is given by the pressure of the fluid at that position plus the dynamic pressure. The second formula gives the volumetric flow rate in m^3/s at a certain length l in meters of the tube as a function of the pressure difference in pa between the ends of the tube, the tube diameter in meters and the dynamic viscosity µ in pa*s.

With:

$$v_i = \frac{Q_i}{A_i} \; with \; A_i = \pi \cdot \left(\frac{d_i}{2}\right)^2$$

Note that i is an index to denote the tube in the different tubes with c for the Coriolis sensor tube and b for the bypass tubes (note that for the bypass tubes the flow needs to be multiplied by the amount of bypass tubes). v is the flow velocity in m/s, A is the crossectional area of the tube in m^2.

Next a pressure balance is made, where the external pressure (which is used to pump the fluid into the tube) is equal to the pressure drop across the tube(s) plus the dynamic pressure:

$$p_{ext} = 2 \cdot (p_{ext} - p_{i,in}) + (p_{i,in} - p_{i,out})$$

Filling the results from Bernouilli's law and Poisseuille's equation into the balance and solving for both tubes yields:

$$\frac{1}{2} \cdot p_{ext} = \frac{64 \cdot \mu \cdot l_c \cdot Q_c}{\pi \cdot (d_c)^4} + \frac{8 \cdot \rho \cdot {Q_c}^2}{\pi^2 \cdot (d_c)^4} = \frac{64 \cdot \mu \cdot l_b \cdot Q_b}{n \cdot \pi \cdot (d_b)^4} + \frac{8 \cdot \rho \cdot {Q_b}^2}{n^2 \cdot \pi^2 \cdot (d_b)^4}$$

Rearranging the equation gives the constraint for the flows:

$$n^2 = \frac{Q_b \cdot (d_c)^4 \cdot (8 \cdot \mu \cdot l_b \cdot \pi \cdot n + \rho \cdot Q_b)}{Q_c \cdot (d_b)^4 \cdot (8 \cdot \mu \cdot l_c \cdot \pi + \rho \cdot Q_c)}$$

This constraint shows that for high flows the ratio is fully determined by the number of tubes, whereas for low flows the length of the tubes also plays a role. For the range of 1 to 10 bars that will be used for measurement the flow is in the transition regime between the high-flow and the low-flow ratio. The reason for this is the transition between turbulent and laminar behavior of the flow.

3.2 Start on gas model

These equations are the ones that are valid for fluids only. For gas some other equations are valid. The major difference lies in its density and its dynamic pressure. The major difference between gases and fluids is that gases are compressible whereas fluids are not. Therefore the dynamic pressure should be replaced by the following expression [aero]:

$$p_{dyn,gas} = \frac{1}{2} \cdot \gamma \cdot p_s \cdot M^2$$

Where M is the Mach number, γ the ratio specific heats for a gas and p_s the static gas pressure. The Mach number is the ratio of the flow velocity of the gas to its sound velocity and therefore the dynamic pressure has a square relation with the flow velocity.

This equation is obtained when the density is replaced by the density according to the ideal gas approximation:

$$\rho = \frac{M_{molar} P}{R \cdot T}$$

M_{molar} is the molar weight of the gas, which is just a property of a material. And R is the universal gas constant. The ideal gas law is used in this case as an approximation to keep the model simple.

To determine the density in this case a value for the pressure has to be taken. To do this the pressure drop across the tubes is assumed to be linear with distance, which is true for a straight tube with laminar flow. Next the average pressure inside the tube is taken, in this case input pressure + output pressure divided by 2 and fill this in as an approximation for the density. This would be a rather easy approximation as both the input pressure (the pressure that you apply) and the output pressure (atmospheric pressure) are known. Therefore the following formula for the dynamic pressure is used:

$$p_{dyn,gas} = \frac{1}{4} \cdot \frac{M_{molar}(p_{ext} - p_{atm})}{R \cdot T} \cdot v_i^{\ 2}$$

In this formula the Mach number and the ratio of specific heats divide the speed of sound out of the equation, resulting in an equation for the dynamic pressure with a similar form as the one for fluids.

Also the dynamic viscosity of a gas is temperature dependent and is given by:

$$\mu = \mu_0 \frac{T_0 + C}{T + C} \cdot \left(\frac{T}{T_0}\right)^{\frac{3}{2}}$$

With T_0 and C and μ_0 properties of the gas, since the temperature is considered to be constant across the chip the dynamic viscosity of the gas is constant. Note that this equation only holds for ideal gases.[gastemp]

3.3 Other causes of deviation

The Coriolis mass flow sensor contains 8 bends which cause an additional pressure loss within the fluid flow. To account for this behavior the equivalent length rule can be used; a straight tube is modeled with tube pieces of certain length replacing the corners. So in other words this modeled Coriolis tube will be longer than the real tube with bends to compensate for the pressure drop within the bends. In the current models for both gasses and fluids the pressure drop due to bends is neglected.[bend]

Other effects that have been neglected in the model but have an impact on the behavior of the chip is the pressure drop across the inlet and the outlet tubes and the valve of the flow controller, turbulent behavior for the gas model and all effects of a changing temperature such as thermal expansion, changing viscosity etc.

4 Chip analysis

4.1 Design analysis

An initial mask design was made for the PRECISE project in Clewin. (See figure 3). The Coriolis tube was designed with a length of 17.28mm while the bypass tube was designed with a length of 0.46mm. Both tubes have an equal diameter; this gives a flow ratio of 37.24 using the low flow approximation of the model. There is also a version of this chip without bypass tube for reference.

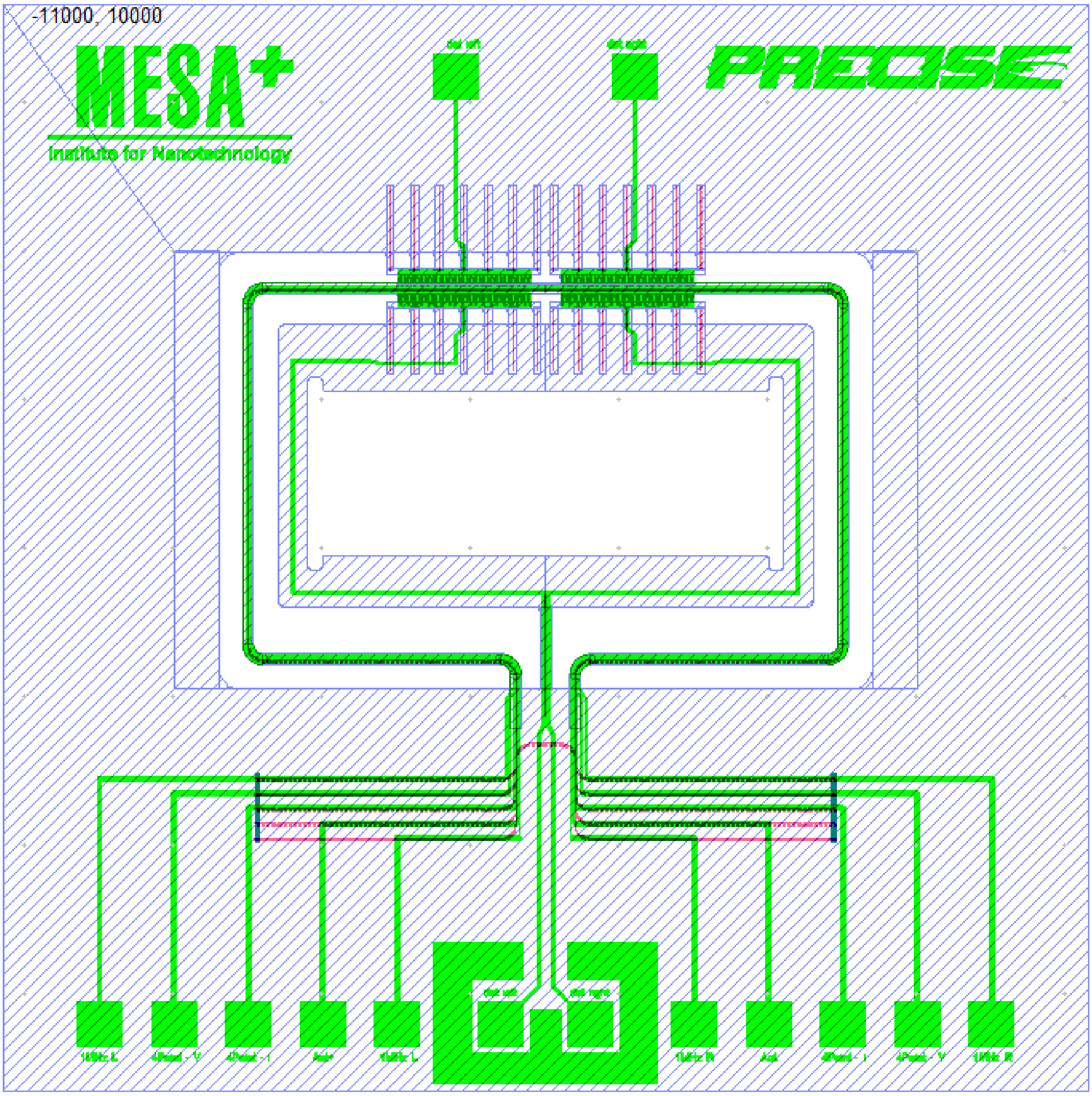

Figure 3: Clewin design of a Coriolis mass flow sensor chip with one bypass tube added

The other designs are made as a part of the F7 series and sport a different buildup, meaning that these should be analyzed separately from the PRECISE project chips. Where the PRECISE chip used only one bypass tube the F7 series used multiple bypass tubes, so that the tubes could be made longer while having in theory the same effect. This way of designing the bypass tubes has a few advantages in comparison with the way the PRECISE chip was designed. The first advantage is that it enables a way to achieve very large ratios such as 1:99. The second advantage is that for larger pressures the flow ratio will be proportional to the amount of tubes, so if the ratio declines when there are 5 bypass tubes in parallel then the ratio will eventually decline to 5, which is still larger than 1:1. A series of chips has been designed with the following ratios:

- The F7 1:17 chip, analysis in Clewin (Coriolis length=16.67mm, bypass length=2.976 mm, ratio=1:16.80) using 3 bypass tubes.
- The F7 1:24 chip, analysis in Clewin (Coriolis length= 15.67mm, bypass length=1.976 mm, ratio=1:23.79) using 3 bypass tubes.
- The F7 1:28 chip, analysis in Clewin (Coriolis length=16.69mm, bypass length=2.976 mm, ratio=1:28.04) using 5 bypass tubes.
- The F7 1:31 chip, analysis in Clewin (Coriolis length=15.18mm, bypass length=1.480 mm, ratio=1:30.77) using 3 bypass tubes.
- The F7 1:40 chip, analysis in Clewin (Coriolis length=15.69mm, bypass length=1.976 mm, ratio=1:39.70) using 5 bypass tubes.
- The F7 1:51 chip, analysis in Clewin (Coriolis length=15.17mm, bypass length=1.480 mm, ratio=1:51.25) using 5 bypass tubes.
- The F7 1:59 chip, analysis in Clewin (Coriolis length=14.45mm, bypass length=0.728 mm, ratio=1:59.54) using 3 bypass tubes.
- The F7 1:99 chip, analysis in Clewin (Coriolis length=14.42mm, bypass length=0.728 mm, ratio=1:99,03) using 5 bypass tubes

These numbers are obtained using the designs in Clewin such as the example in figure 3. These have been done so that the accuracy of the models for the different chips can be increased, improving the accuracy of the predictions.

4.2 Behavior analysis

The simulations show that the decline in ratios start for each chip the same point and end approximately by the same point in terms of mass flow, the problem of this is that it implies that the higher the intended ratio the faster the decline. In all these plots the dynamic viscosity of water is taken and is $^{10-3}$ Pa*s. This is quite evident in the pressure inlet plots of figure 4 and 5:

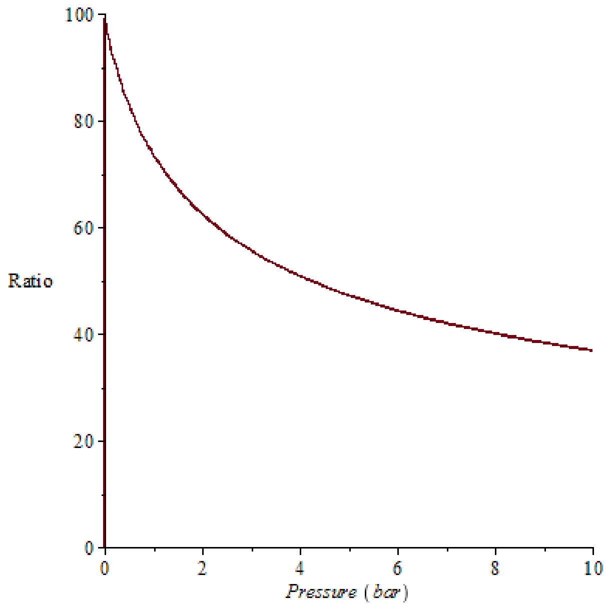

Figure 4: F7 1:99 chip modeled with water using the constraint from my model.

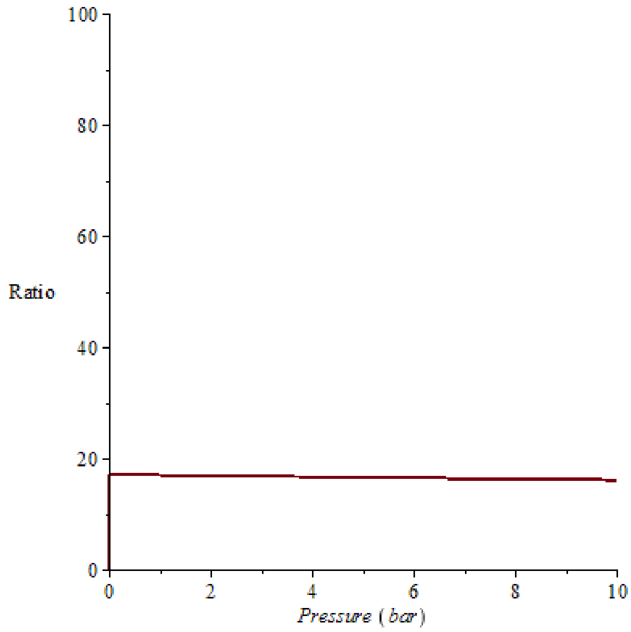

Figure 5: Coriolis mass flow sensor chip designed with a bypass-Coriolis ratio of 17 using 3 bypass tubes

A remedy to this however is to make the ratios at high flow and low flow closer together, this can be done by increasing the amount of tubes. By doubling the tubes for example you halve the decay in ratio. What also helps is to keep the ratio low, which is basically altering the starting ratio. The effect can be seen in figure 6 where the same ratio as in the first is achieved with twice the amount of tubes:

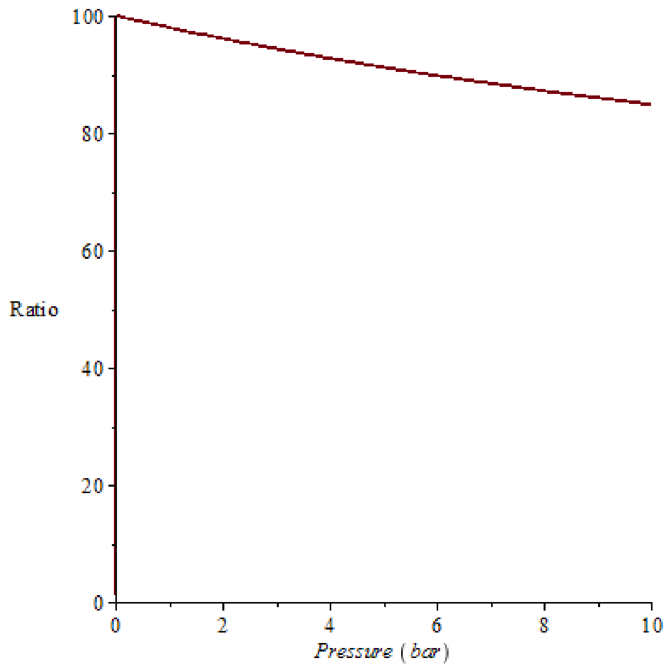

Figure 6: Model of the F7 1:99 chip with 10 tubes instead of 5 tubes

The pressures at which the ratios have declined to 95 % of their original value are listed in table 1:

17	1.52 bar
24	0.91 bar
28	1.52 bar
31	0.56 bar
40	0.91 bar
51	0.56 bar
59	0.14 bar
100	0.14 bar

Table 1: A table with in the left column the designed chip ratios and in the right column the pressure at which the ratios have declined to 95% of their original ratio as predicted by the model.

Based on these calculations and simulations the advice can be given to achieve the intended ratio by using a larger number of tubes instead of a large tube length ratio.

5 Measurements

5.1 Set-up

To test the model measurements are performed. To make the measurements the set-up in figure 7 is used.

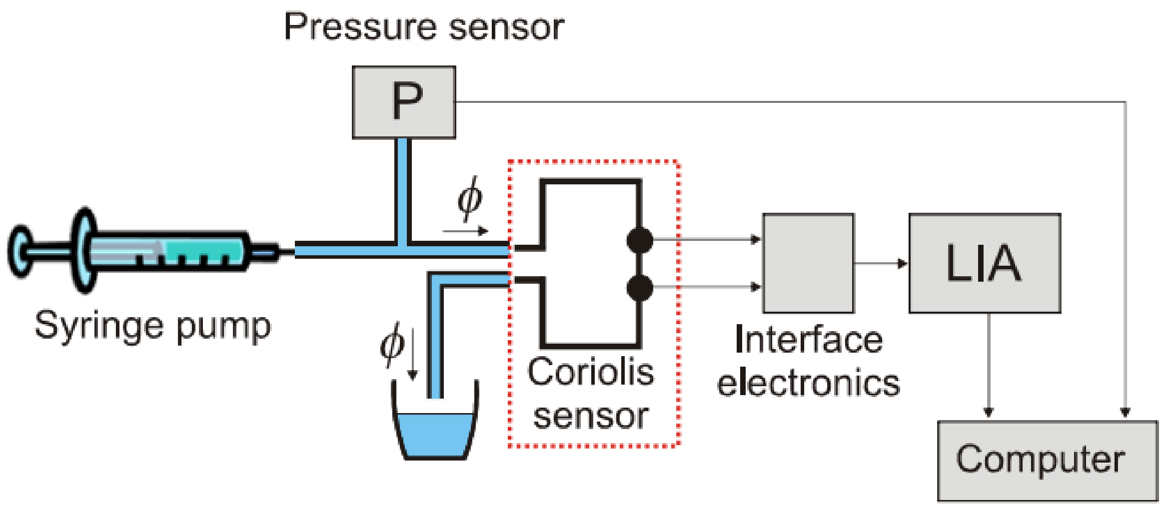

Figure 7: Overview of the flow measurement set-up. A lock-in amplifier is used for detecting the phase shift of the sensor output signals

The measurement process will go in the following way: A certain mass flow is inserted into the chip, while being measured by the reference sensor which is combined with the pressure sensor in this graph. The capacitors measure the phase shift in the actuation signal and the output signal. The phase shift combined with the flow data is used to determine the sensitivity of the chip in degrees per phase shift, which is then compared with a reference chip. The reference chip will be a chip with the same Coriolis tube, but without the bypass tubes.

The reference sensor was measured with this set-up, but later a different set-up was used as depicted in figure 8. In this set-up a flow controller is used which is controlled by the computer, so now all equipment is controlled in one program on the computer making the process more efficient. The flow controller also keeps the flow more steady then the step motor of the pump used in the previous set-up. A disadvantage is that there is a lot of pressure drop over the controller equipment, this combined with the limitation of the gas inlet used to create the pressure, limits the maximum pressure to 8 bar and the flow to certain values depending on the chip.

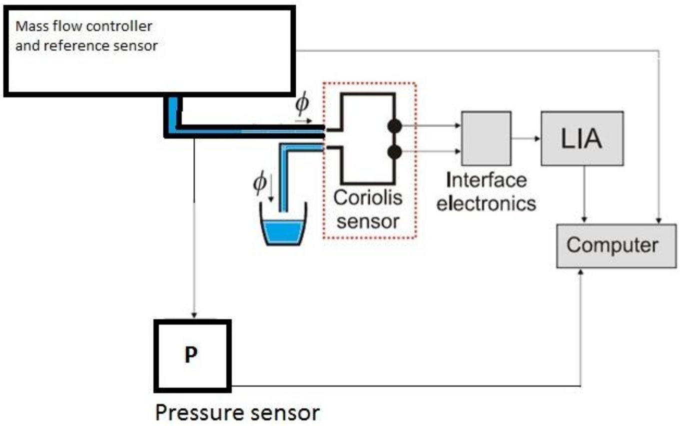

Figure 8: Overview of the new flow measurement set-up. A lock-in amplifier is used for detecting the sensor output signals

5.2 Measurement plan

Measurements will be done using the earlier described set-up and will be done for each chip separately.

The entire system measures a whole range of parameters:

- Phase shift between actuation and capacitor read-out signals, which is a measure for the mass flow in the Coriolis tube.
- The pressure, which is measure so the relation between flow and pressure can be found.
- The reference mass flow

Before the measurements are started using the chips with bypass tubes a normal Coriolis mass flow sensor is measured to determine the sensitivity of the Coriolis tube sensor. This sensitivity will be expressed in degrees phase shift per mass flow (g/hr). This sensor has been designed for a flow of 1 g/hr for 1 bar pressure. For low flows the pressure and the flow are linearly proportional for example 2 g/hr is approximately 2 bars. If now a chip is used with bypass tubes designed for a certain ratio this flow range is multiplied with this ratio. A chip designed with a bypass-Coriolis ratio of 1:17 can handle 18 times as large flows and has a flow of approximately 36 g/hr for 2 bars applied if the ratio stays constant. So at 36 g/hr the 1:17 chip should have the same amount of phase shift as the normal sensor has at 2 g/hr. For these chips the sensitivity can also be determined in degrees phase shift per mass flow. If it is assumed that the sensitivity of the Coriolis tube is constant then using the reference flow the ratio between bypass flow and Coriolis tube flow can be determined.

To determine all these results Matlab will be used to calculate the flows and plot them so that a sensitivity plot is obtained and finally the ratio plot that can be compared with the predictions.

So the measuring scheme for each chip is as follows

- The valve of the flow controller is completely opened.
- The maximum flow that the chip reaches will be taken as the largest setpoint
- An evenly spaced interval of flow setpoints is made

- 0-flow points are put between these setpoints to easily distinguish them and to determine the offset in the data.

After the measurement for each chip the sensitivity of each chip will be determined and with that data the behavior of the flow ratios is calculated. From the data the pressure drop over the inlets and outlets is determined and used to correct the data for the Flow-pressure graphs

Pressure is lost in the inlet and the outlet tubes of the chip and the valve of the flow controller and there is a pressure deviation from the measurement itself. To account for this deviation after measurements the Hagen-Poiseuille equation shall be used to calculate the pressure drop of these tubes. This pressure drop is used to correct the measurement data of the pressure at the measurement. The Flow measurement data shall be used to this end

5.3 Expectations

All chips show the same type of behavior and the decay is something which can be easily measured and used to verify the model. For each chip 10 ratios are calculated for 10 different inlet pressures, which will be compared with the measurement results. Underneath the bypass flow to Coriolis flow ratios for the F7 chips as predicted by the model are listed in table 2:

Chip ratio in design	Ratio at 1 bar	Ratio at 2 bar	Ratio at 3 bar	Ratio at 4 bar	Ratio at 5 bar	Ratio at 6 bar	Ratio at 7 bar	Ratio at 8 bar	Ratio at 9 bar	Ratio at 10 bar
17	16.33	15.92	15.54	15.20	14.88	14.59	14.33	14.08	13.85	13.63
24	22.69	21.63	20.74	19.98	19.31	18.72	18.20	17.73	17.30	16.90
28	27.22	26.53	25.90	25.33	24.81	24.32	23.88	23.46	23.08	22.71
31	27.57	25.77	24.35	23.19	22.21	21.36	20.63	19.98	19.40	18.87
40	37.82	36.05	34.57	33.29	32.19	31.21	30.33	29.55	28.83	28.17
51	45.92	42.95	40.58	38.64	37.00	35.61	34.38	33.30	32.33	31.45
59	46.24	39.73	35.62	32.68	30.44	28.65	27.18	25.93	24.85	23.92
100	77.06	66.21	59.36	54.47	50.74	47.75	45.29	43.21	41.42	39.86

Table 2: Bypass-Coriolis ratios for different pressures for the F7 chips as predicted by this model

The same was done for the PRECISE bypass chip in table 3:

Chip ratio in design	Ratio at 1 bar	Ratio at 2 bar	Ratio at 3 bar	Ratio at 4 bar	Ratio at 5 bar	Ratio at 6 bar	Ratio at 7 bar	Ratio at 8 bar	Ratio at 9 bar	Ratio at 10 bar
37.24	21.14	16.84	14.53	13.01	11.91	11.06	10.38	9.82	9.35	8.95

Table 3: Bypass-Coriolis ratios for different pressures for the PRECISE bypass chip as predicted by the model

The earlier observation that a smaller tube length ratio and a large amount of tubes would lessen the decrease in ratio as the pressure is increased can be clearly seen in the predictions as the flow ratio of the PRECISE chip decreases fast at 1 bar of pressure applied already.

6 Results and the evaluation of the measurement data

Measurements were done on the following chips:

- The F1 chip without bypass tubes, this chip has the same Coriolis tube as the F7 chips and is intended to be used as a reference chip.
- The F7 1:99 chip.
- The F7 1:24 chip.
- The F7 1:40 chip.
- The PRECISE chip without bypass tube.
- The PRECISE chip with one bypass tube (1:37.24).

A preliminary evaluation of the measurement data shall be done in this chapter

6.1 PRECISE chip with bypass tube

The measurement results in figure 9 were obtained during measurements using the PRECISE chip with bypass tube:

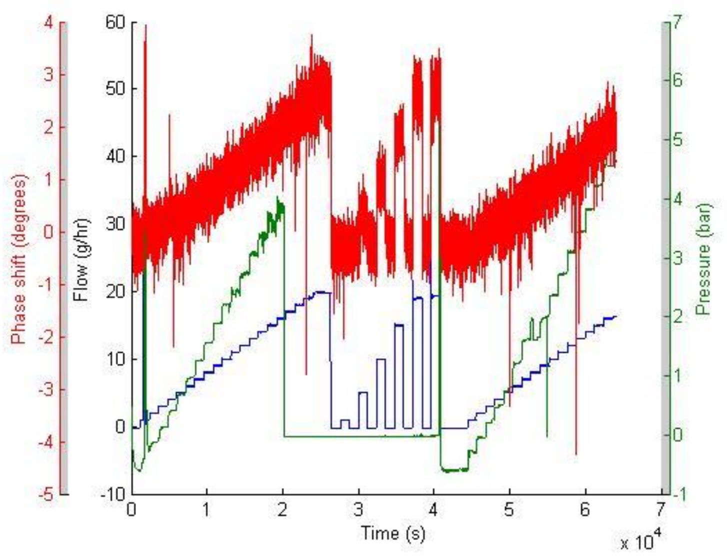

Figure 9: Measurement data from the PRECISE bypass chip.

As can be seen the signal is clearly dependent on the flow and pressure. The pressure sensor however doesn't work from t=20000 onwards until the cycle starts anew at approximately t=40000. This has as a consequence that the data before t=20000 needs to be used for a more complete analysis of the chip behavior as that seems to give the most complete overview.

What can be seen from the phase shift in the signal is that it contains a lot of noise around the actual values belonging to the respective setpoints. To correct for this behavior the average is taken for each setpoint. Overall the data looks like something that can be expected from this chip. The data is suited for analysis of the chip behavior. What is striking is that the response seems to be quite linear, while the ratio between the Coriolis flow and the bypass flow should decrease from 1:37 to 1:11. This seems to indicate that the ratio remains constant over the measurement.

6.2 PRECISE chip without bypass tube

The measurement data in figure 10 was obtained during measurements on the PRECISE chip without bypass tube:

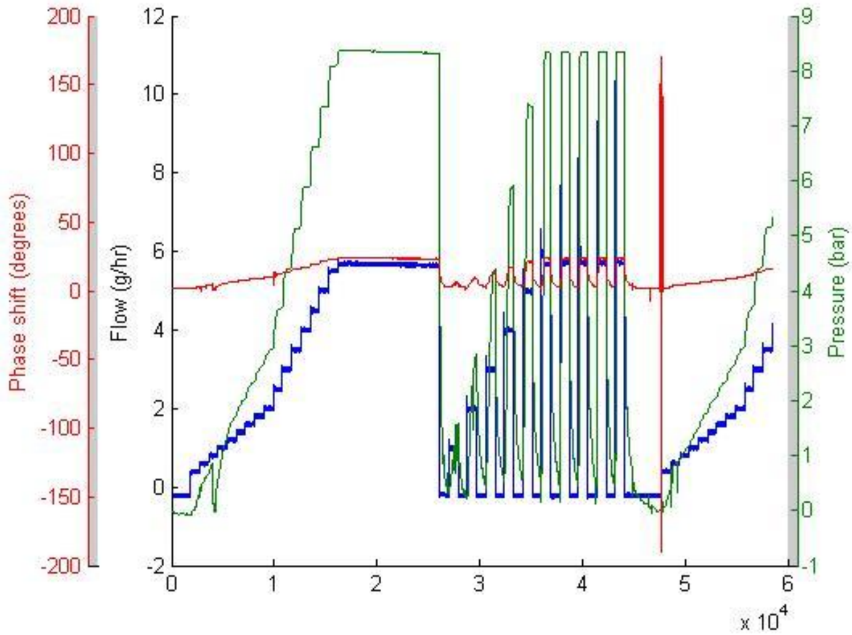

Figure 10: Measurement data from the PRECISE chip without bypass.

All of the signals seem to follow each other almost linearly, but what is seen during the setpoints early on in the measurement is that the pressure builds slowly in the measurement. For the analysis stable setpoints will be used as they give more accurate results.

For the analysis the setpoints from t=10000 until the flow clips are used since the setpoints contain larger steps and are therefore easier to distinguish from each other.

Overall the data seems very sharp and little noise is present resulting in suitable material to perform an analysis on.

6.3 F1 reference chip without bypass

Underneath in figure 11 you can see the measurement data from the F1 chip:

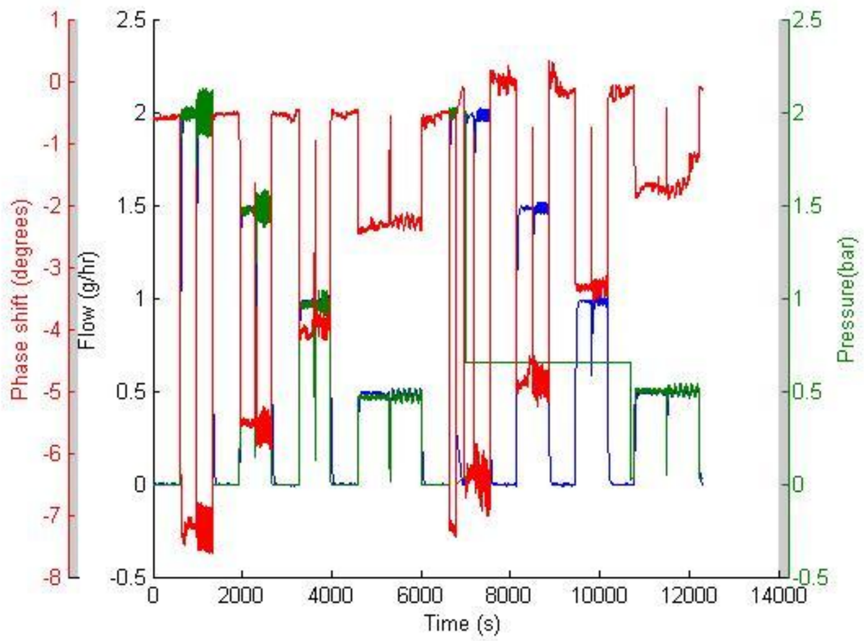

Figure 10: Measurement data from the F1 chip.

This is the only measurement that has been done using the set-up with the pump. The behavior of the pump can be seen in the behavior of pressure, flow and the phase shift during the set-up. The change in behavior halfway the setpoint is because the pump behaves differently when the pump direction changes as the flow direction is kept constant, resulting in non-steady behavior during the second half of the setpoint.

While the data behaves as expected, the data is still of no use for the research because it is measured using a different set-up. This set-up has different lengths of tubes before the sensors and not the unknown pressure drop over the valve; therefore there are too many unknown differences to compare the data of this chip with the data of the other chips. Otherwise this data would have been used to compare the F7 chips with to understand their behavior.

If this data would have been used the average outputs of each setpoints would have been taken and used to make linear fits to which you can compare the F7 chips.

6.4 F7 chip with ratio 1:24

The next batch of measurement data in figure 12 is from the F7 1:24 chip:

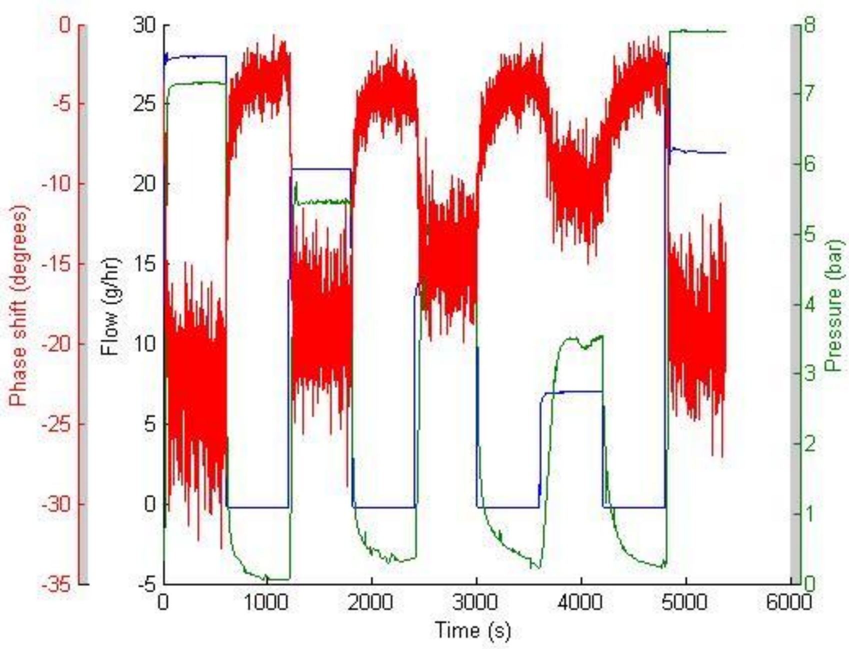

Figure 12: Measurement data from the F7 1:24 chip.

Although the pressure data and the flow data from the reference sensor seem clean, the same cannot be said about the phase shift data. The phase shift data seems to oscillate around an equilibrium point for the different setpoints, so the average for the output data for each setpoint will be taken and analyzed to gain insight into the behavior of the chip.

In figure 13 the phase shift data has been left out to allow a clearer look at the pressure and flow data:

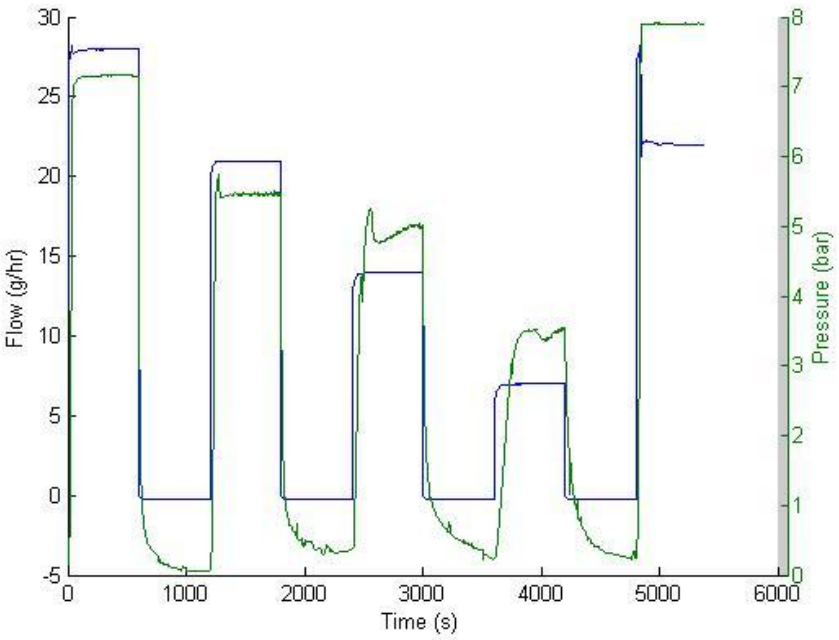

Figure 13: Measurement data from the F7 1:24 chip without the phase shift data

What can be seen is that the pressure data doesn't behave quite linear in relation to the flow. A line can be drawn through the pressure setpoint data, but the middle 2 setpoints do not lay exactly on the line. This non-linearity however is not unexpected as a chip with bypass tubes shifts ratios for higher flows, so that the relation between flow and pressure should be non-linear. To make a better analysis averaging is clearly needed.

The pressure data has some bumps in the third and fourth non-zero setpoint, which is something that may cause deviations in the analysis when the data is averaged over the setpoints. Therefore caution must be taken when this data is analyzed.

6.5 F7 chip with ratio 1:40

Another chip that was measured was the F7 1:40 chip with its data present available in figure 14:

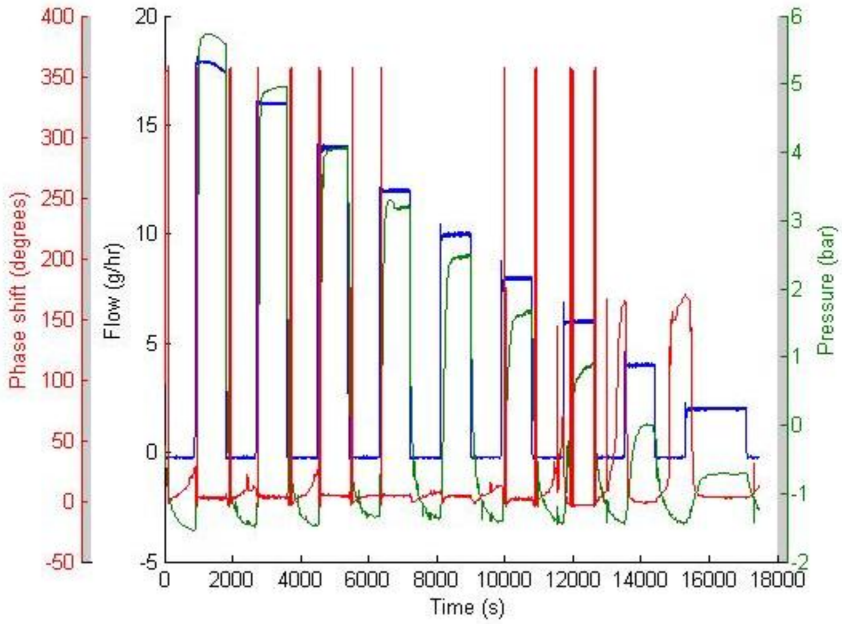

Figure 14: Measurement data from the F7 1:40 chip.

There is a large offset in the pressure due to not starting the measurement exactly at P=0, which is something that can be fixed by adding the offset. This problem is present at all measurements and also will be fixed for the analysis of all the other chips. The flow and the pressure seem to follow the setpoints nicely; the difference in slope may be due to the scale of the axes.

The Phase shift signal however is largely distorted and very low, save for some sudden large peaks, this means that something is wrong in that data and therefore no signal analysis can be made. Even when the peaks are left out of the data in figure 15 the phase shift data still doesn't follow the pressure and flow. This essentially makes the measurement data useless as this is a crucial part in the analysis of the chips.

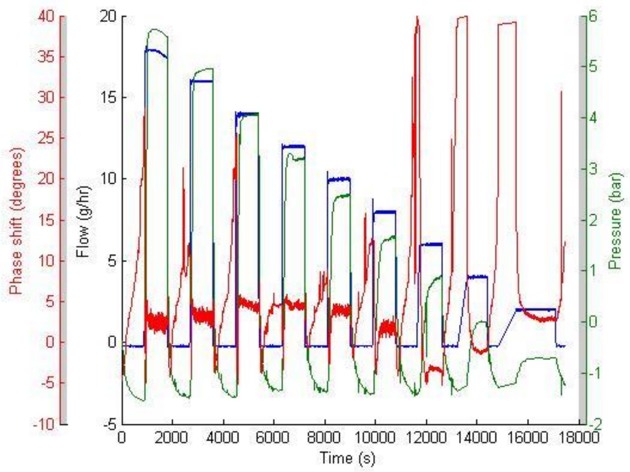

Figure 15: Measurement data from the F7 1:40 chip with some clean up.

6.6 F7 chip with ratio 1:99

The last chip that was measured was the F7 1:99 chip with its measurement data listed in figure 16:

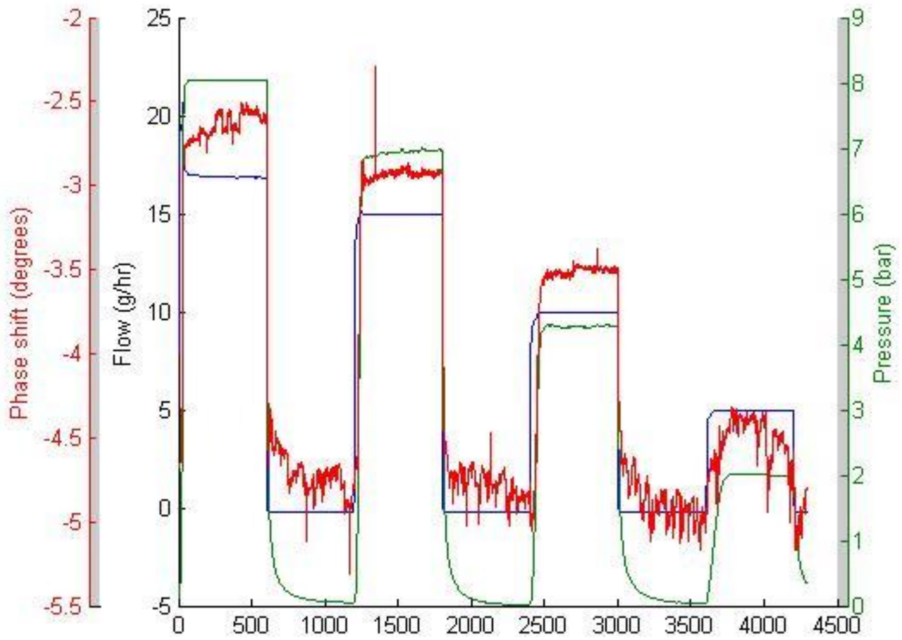

Figure 16: Measurement data from the F7 1:99 chip.

The first setpoint was set at a higher point, but the pressure wasn't high enough to reach the flow causing the flow to clip at around 18 g/hr. When that is taken into account all the signals seem to behave in a linear manner, which is expected behavior for such a chip.

The data from the phase shift signal contains some noise when there is no flow present. From the setpoints the averages will be taken to analyze the data just as was done for all the other chips.

7 Analysis and discussion of the measurement data

7.1 Ratio analysis PRECISE bypass chip

7.1.1 First analysis measurement data

To reduce the amount of measurement points that have to be dealt with the average of each setpoint in terms of flow, pressure and phase shift was taken and processed into two plots: In figure 17 the phase shift of both chips is plotted against the flow and in figure 18 the flow of both chips is plotted against the pressure. This is done because for the logical reason that a pressure causes a flow causes a phase shift in the signal.

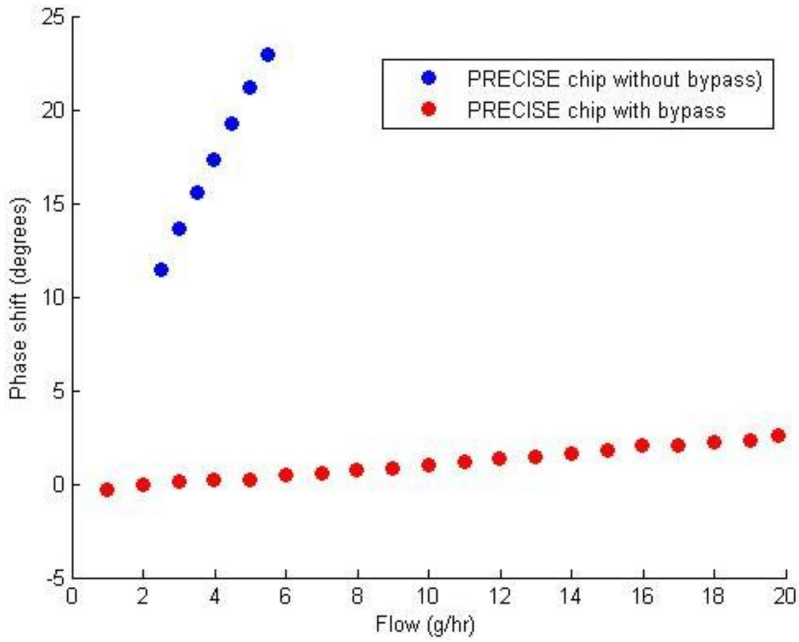

Figure 17: Scatter plot of the phase shift against the flow for the PRECISE chips.

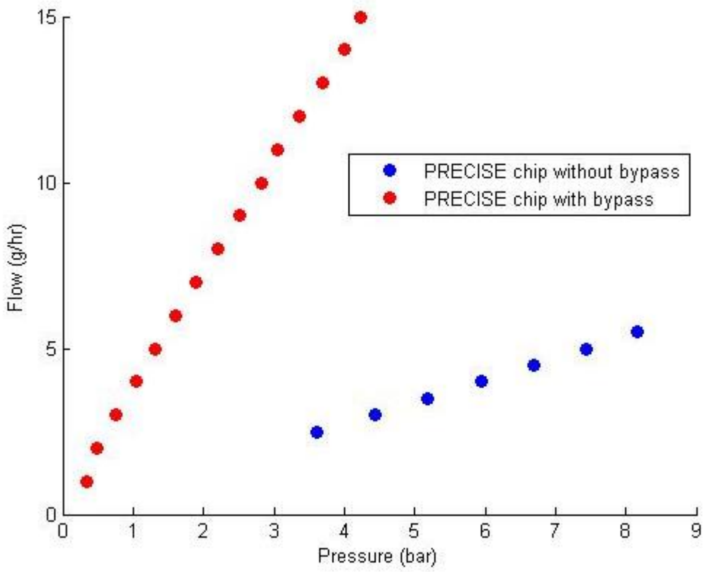

Figure 18: Scatter plot of the flow against the pressure for the PRECISE chips.

In both of these plots you can see that both chips show linear behavior. The reason why there are no setpoints near 0 bar pressure for the chip without bypass is that those were difficult to identify and the setpoints that were clearly stable were taken. To compare the data from the chip with bypass to the data from the chip without bypass a linear fit will be made from the data without bypass since this is the most linear data and makes comparing easy.

The ratio between the two chips is equal to the ratio of the slopes of the phase shift flow data. So for the ratio the following formula will be used:

$$ratio = \frac{a_{wb}}{a_{byp}} = \frac{a_{wb}}{\frac{ps_{i+1} - ps_i}{f_{i+1} - f_i}}$$

Where a_{wb} is the slope of the phase shift-flow graph for the chip without bypass determined using the linear fit function in Matlab. a_{byp} is the slope of the phase shift-flow graph for the chip with bypass, ps_i is the phase shift, while the index i stands for the index number of the measurement point and finally f_i is the flow belonging to that measurement point. This ratio will be plotted against the average flows on these intervals which are determined using the following formula:

$$f_n = \frac{1}{2}(f_{i+1} + f_i)$$

After applying these formulas the resulting data is plotted in figure 19:

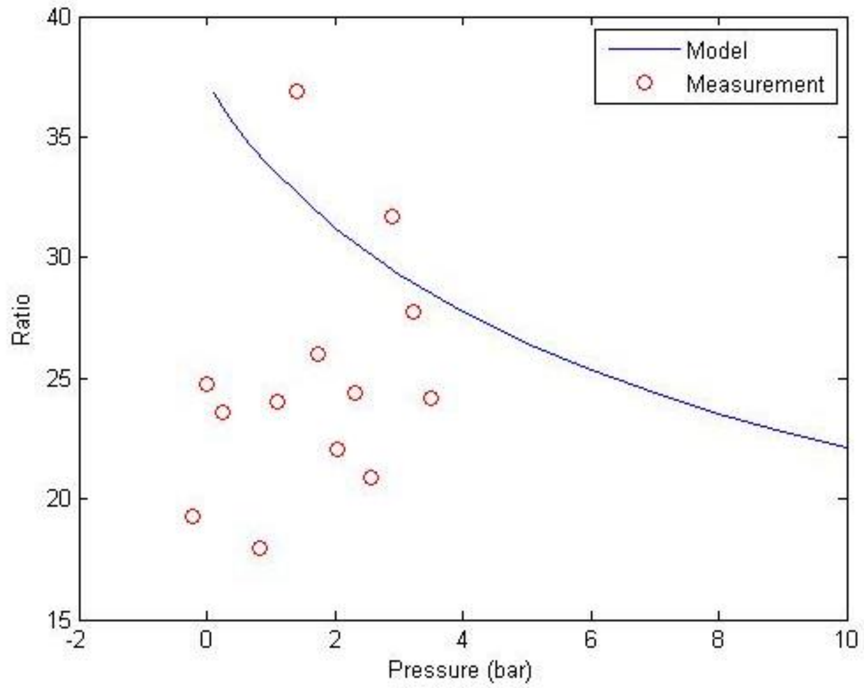

Figure 19: A plotting of the ratios of signals between the different chips as determined from the signal-flow graph. The line of the ratio from the model is also present.

This above graph contains the ratios as determined from the signal-flow graph as a function of the input flow. A point in this graph which was a lone bump at a ratio of -130 was left out of the analysis. This point deviated a lot from the other points due to small fluctuations in the signal data resulting in a slightly lower signal in comparison with its previously measured point resulting in a negative slope. This point deviated so much in comparison with the other points that it was left out of the graph and the rest of the analysis. What can be seen from this graph is some variation between a ratio of 18 and 36 around 25 for this chip. Next a similar analysis of the flow-pressure graph was done, which resulted in the graph in figure 20:

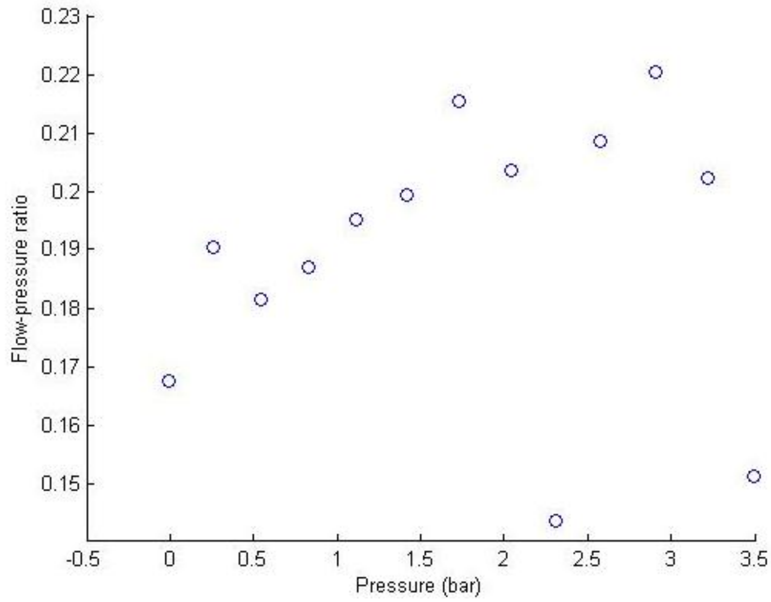

Figure 20: analysis of the ratio of flows of the chips as made from the flow-pressure graphs

From this the same behavior as in figure 19 can be seen but on a much lower scale.

7.1.2 Comparison with model for flow-pressure characteristic

First the flow-pressure graph of the PRECISE bypass chip (Figure 21) will be compared with the model (Figure 22).

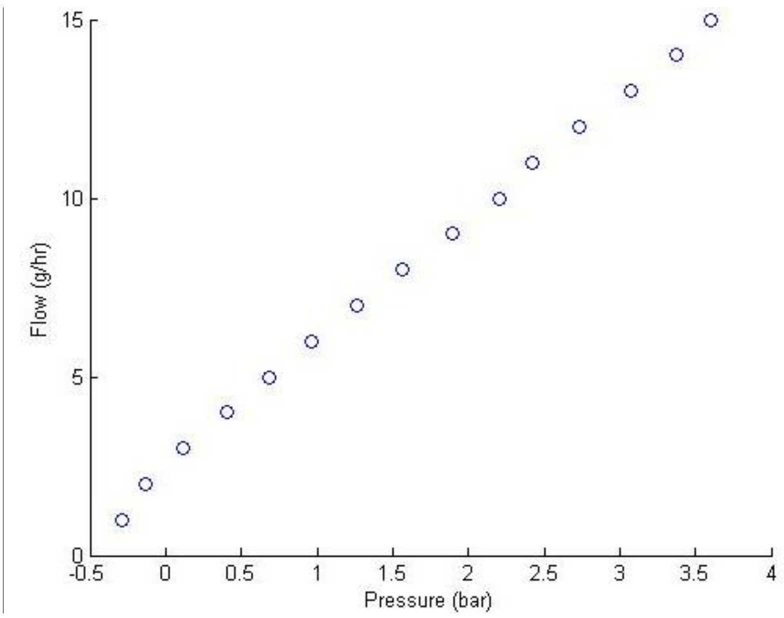

Figure 21: Flow(g/hr)-pressure(bar) graph as measured in the PRECISE chip with bypass

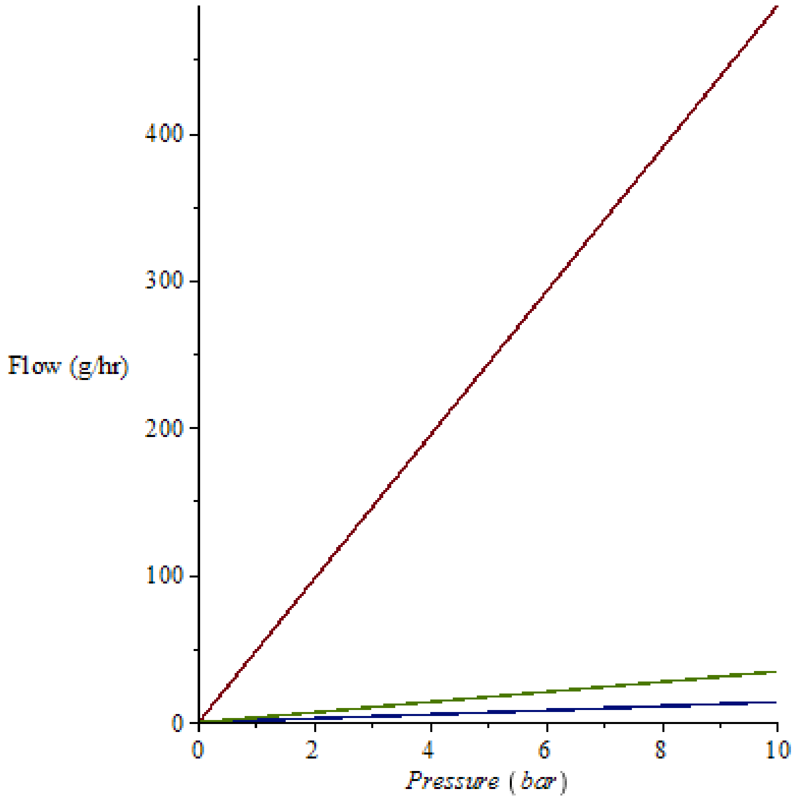

Figure 22: Flow(g/hr)-pressure(bar) graph as predicted by the Maple model. Red line is bypass flow, blue line is Coriolis flow and the green line is the flow as measured by the reference sensor

As can be seen from the graph there is quite some difference on the matter of scale, this is due to the extra pressure losses of the inlet and outlet tubes into the chips and the pressure drop over the valve of the flow controller.

To cope for this Hagen Poisseuille's equation is used to correct for the pressure losses of the tubes other than the Coriolis and bypass tubes. But to do that the equation will be rewritten to calculate ΔP:

$$\Delta P = \frac{128 \cdot 10^{-5} \cdot \mu \cdot l}{\pi \cdot d^2} \cdot Q$$

Filling in the data: For all the chips have 250µm diameter for the external tubes with a combined length of 82 cm. For water a dynamic viscosity µ of 10^{-3} Pa*s is used. The internal tube dimensions are different and the diameter for all the chips is 40 µm and the length for the PRECISE chip is 1.66 mm. Using this equation on all the measurement points produces the following plot:

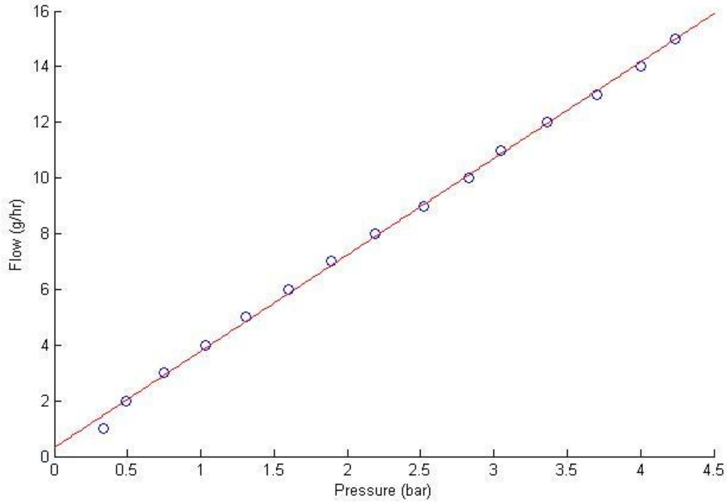

Figure 23: Adapted Flow pressure graph from the measurement data of the PRECISE chip

The results show that remarkably little pressure is lost over the inlet and the outlet tubes of the chip as the differences were in the order of several hundreds of nanobars pressure. The slope of this data according to the linear fit is exactly the same as the one before correction because the linear fit is precise up to 4 decimals. This could indicate together with the large deviation in the model that the large pressure difference is made somewhere else in the measurement set-up. This observation will be compared with the results of the other bypass chips.

7.1.3 Comparison with the ratio prediction

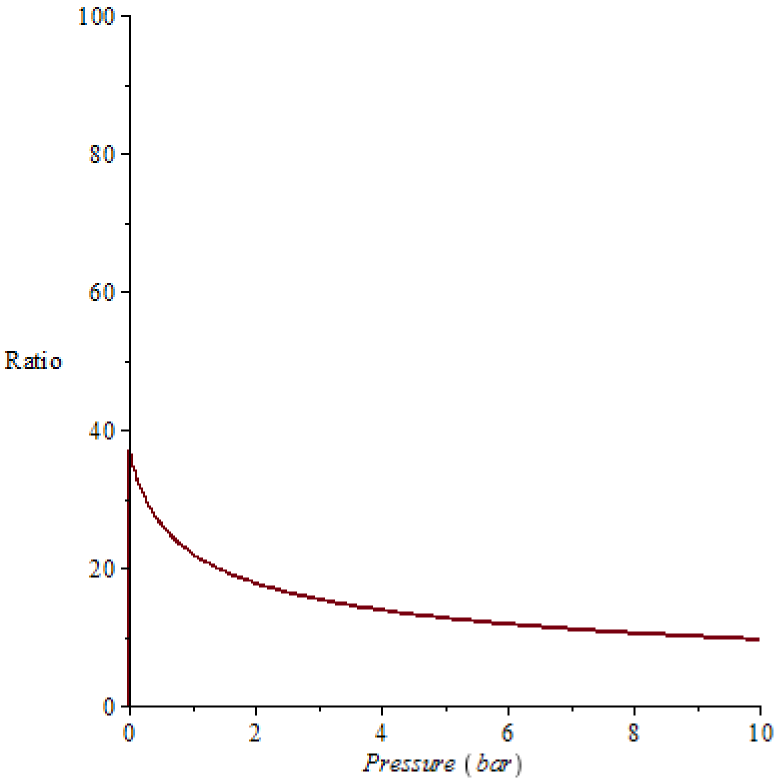

Figure 24: The ratio as a function of the pressure as predicted by the model

The ratio according to the measurement is up and around 27. If this is compared with the prediction made by the model in figure 6 then the first thing that comes in mind is what the ratio change is in the measured interval according to the model. After checking the model the ratio is 31 at 2 bar and 23.5 at 8 bar pressure, which means that the ratio as predicted and the ratios calculated are in the same range. The average ratio as taken from the phase-shift-flow graph is 27. If this value is filled into the model this ratio is reached at a pressure of 4.5 bars which is approximately the average pressure of the pressure range. There is a lot of deviation however as the ratio does not seem to decline when the flow is increased. This is also evident from the raw data as it seems quite linear, however the ratio should decrease drastically. The ratio seems to remain constant and therefore the only thing that matches is the average ratio.

7.1.4 Discussion of the model after the PRECISE chip analysis

The average ratio is predicted approximately right by the model, but it seems to vary around a constant equilibrium point over the flow range and therefore the pressure range. This deviation may be explained by the small oscillations present in the behavior of the flow controller, which can be seen from other experiments. These deviations when used to compare to a constant slope determined from a linear fit result in quite some deviations. This is due to the way in which the calculation is done. There seems to be a large factor difference between the flow-pressure characteristic as predicted by the model and the real measurement results. Comparison with other results can say more about this factor and the validity of the model on this part.

7.2 Ratio analysis F7 chips

7.2.1 First analysis measurement data

The measurement data of the F7 chips will be analyzed in this section. Once again the amount of data points has been reduced by taking the averages of the setpoints in terms of flow, pressure and phase shift and two plots were made: What was done for the PRECISE chips is also done over here: in figure 25 the phase shift of both chips is plotted against the flow and in figure 26 the flow of both chips is plotted against the pressure.

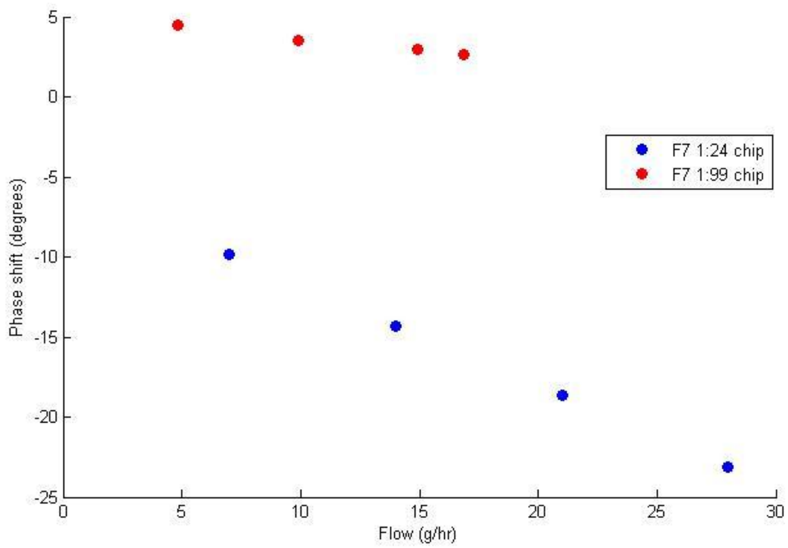

Figure 25: Scatter plot of the phase shifts against the flow for the F7 chips.

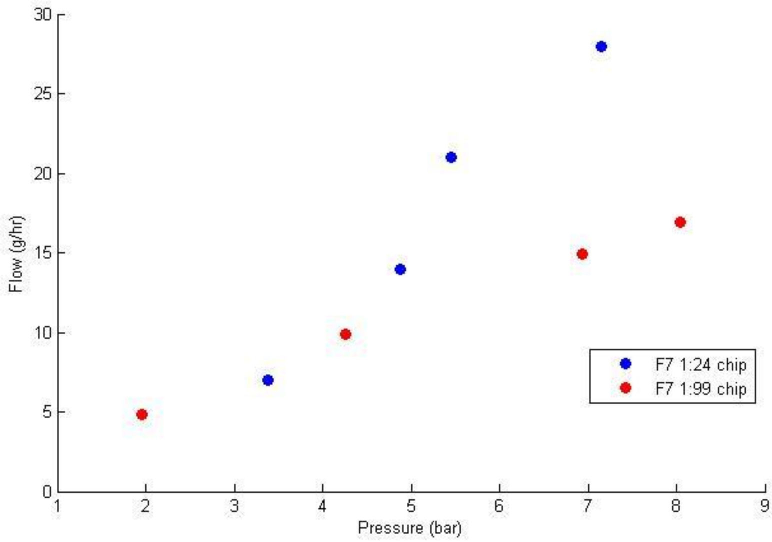

Figure 26: Scatter plot of the flow against the pressure for the F7 chips.

Like the PRECISE chips both F7 chips also show linear behavior in terms of flow and phase shift. The 1:24 chip deviates quite a bit from linear behavior in the flow-pressure graph; this is because of the earlier measured bumps in the pressure at the setpoints. Again the setpoints at 0 bar pressure have been left out due to the data being unstable. This time however the ratios of the chips with respect to each other will be determined due to the lack of proper measurement data of the F1 chip which is needed as a reference to determine the ratio and compare it with the model.

The ratio between the two chips is equal to the ratio of the slopes of the phase shift flow data. Since these chips have been measured on different flow setpoints a linear fit will be made of the two graphs which will be used to determine the ratio between the chips. So in this for the ratio the following formula will be used:

$$ratio = \frac{a_{24}}{a_{99}}$$

Where a_{24} is the slope of the phase shift-flow graph for the F7 1:24 chip. a_{99} is the slope of the phase shift-flow graph for the F7 1:99 chip. Since only the total ratio is considered one value will come out. The slope of the 1:24 chip is -0.62541 degrees/(g/hr) while the slope for the 1:99 chip is -0.15141 degrees/(g/hr) according to the linear fit option in Matlab.

Applying this formula yields as a result a ratio of 4.147.

Next a similar analysis of the flow-pressure graph was done. In figure 27 the 1:24 chip has a slope of 5.7081 (g/hr)/bar and the 1:99 chip has a slope of 1.9799 (g/hr)/bar yielding a ratio of 2.883 between the two chips. This difference is caused by the fact that a large amount of pressure is lost over other things than the chip resulting in a seemingly larger pressure drop for larger flows, while it is in fact lower

7.2.2 Comparison with model for flow-pressure characteristic

First the flow-pressure graph of the F7 1:24 chip in figure 26 will be compared with the model as pictured in figure 27:

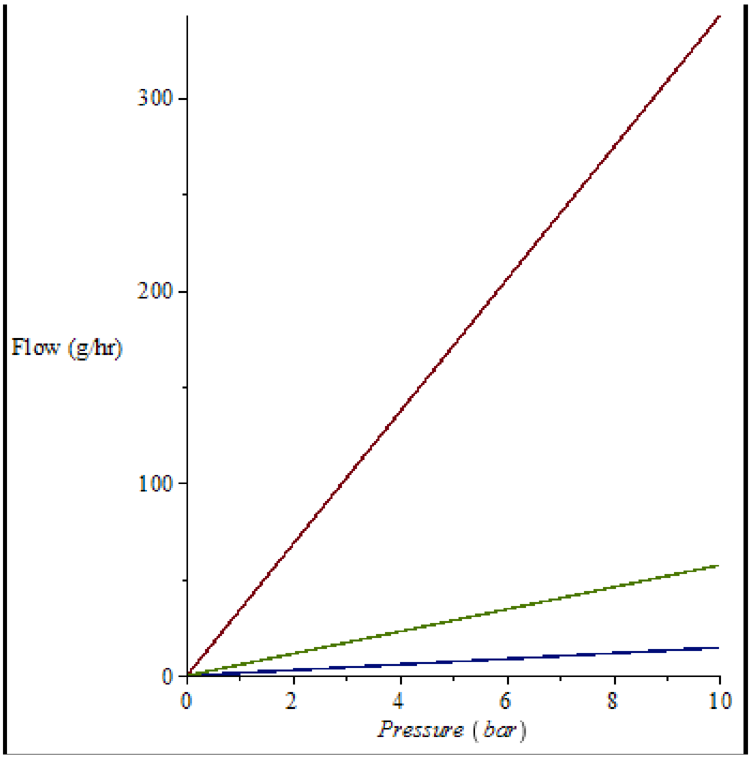

Figure 27: Flow(g/hr)-pressure(bar) graph as predicted by the Maple model for the F7 1:24 chip. Red line is bypass flow, blue line is Coriolis flow and the green line is the flow as measured by the reference sensor

As can be seen from the graph there is quite some difference on the matter of scale, from trying to fit the line in the model it was found that the slope of the model is approximately 6 times as high as the measurement data pointed out.

For this chip it was also tried to improve the results by correcting the pressure data for the inlet and outlet tubes. The difference however was in the order of nanobars and is not shown here as the graphs have not visibly changed.

The same analysis was also done for the 1:99 chip of which the graph is presented in figure 28:

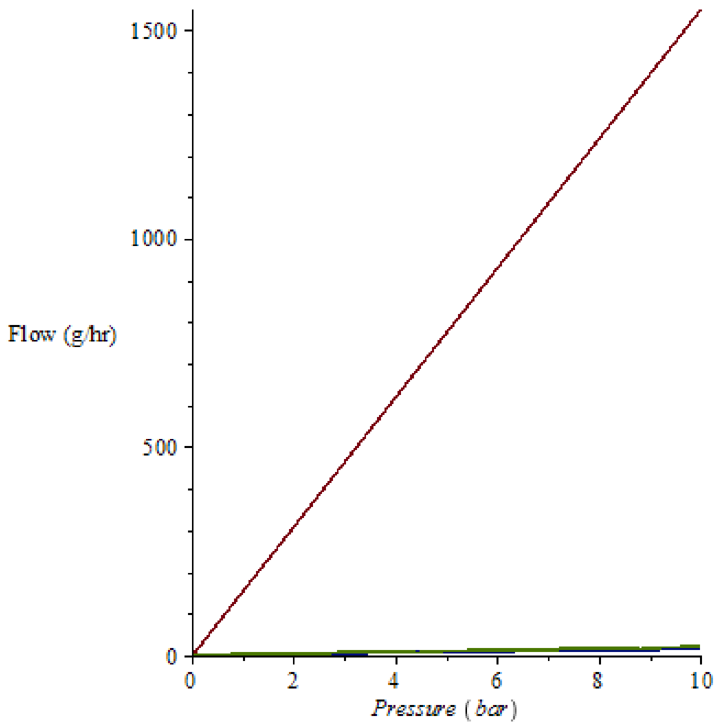

Figure 28: Flow(g/hr)-pressure(bar) graph as predicted by the Maple model for the F7 1:99 chip. Red line is bypass flow, blue line is Coriolis flow and the green line is the flow as measured by the reference sensor

As can be seen the scales of the lines of the measurement data and the Coriolis flow are completely overshadowed by the scale of the line of the bypass flow. After some analysis of the model it was found that the line of the bypass flow is about 80 times as steep as the line of the measurement data.For both chips the tube diameter in the model has been adjusted to see if it had any effect on the outcome of the model. The changing of these 2 parameters had no visible effect on the data from the models.Also the same correction was tried as with the PRECISE chip, but as again the difference was negligible, in the order of nanobars, the result is not shown here as it would give for both chips the exact same Flow-pressure graphs.

7.2.3 Comparison with the ratio prediction

The ratio between the 2 chips was predicted to be around 4, since that is the ratio between 24 and 99, the ratios that the chips were designed with. In that sense the chips behave as expected with respect to one another as their behavior has the same ratio as their ratios with which they were designed.

7.3 Verdict on the flow-pressure graph of the model

Each of the measurements has pointed out a large difference between the slope of the bypass flow from the model and the slope from the reference flow as determined from the measurements. The fact that this factor differs much across the chips and in a non-logical way seems to indicate that a mistake has been made along the lines of the model. Although the pressure drops over the inlet tubes was neglected in the model, the difference isn't as large as would be expected. Therefore the pressure drop is over a different part of the set-up, probably the valve of the flow controller.

8 Conclusions and recommendations

In this report a model was made to describe the behavior of a Coriolis mass flow chip with bypass tubes. On the work done in this report a conclusion will be drawn with regards to the project. Aside from these conclusions there will also be made some recommendations on later research that the University of Twente could perform in the future on the Coriolis mass flow chips with bypass tubes

8.1 Conclusion

The goal of this project is to make and test a model that predicts the behavior of Coriolis mass flow sensors with bypass tubes added.

8.1.1 Modeling

- A model describing the fluid flows in Coriolis mass flow sensor with bypass tubes was made on the basis of the Hagen-Poisseuille's equation and Bernoulli's law.
- A start was made on a model to describe gas flows in the same chips by changing the parameters including a pressure-dependent density and the dynamic viscosity of gases.
- Some efforts have been made to identify sources of deviation in the model.
- These have been put together in two maple files.

8.1.2 Chip analysis

- The chips of the PRECISE project and the F7 project have been analyzed
- This data is used to predict their behavior so that it can be used to compare the measurement data with.
- An analysis using the model has been done to try to give an advice on how to improve the behavior of the chips for more constant flow ratios.

8.1.3 Measurements

- Measurements have been done on the F1 chip, the F7 1:24, 1:40 and 1:99 chips as well as the PRECISE chips; one with bypass tube and the other without bypass tube.
- All data except the ones for the F7 1:40 chip and the F1 chip could be used for analysis

8.1.4 Analysis measurement data

- The ratio of the flows in the PRECISE chip with bypass tube is approximately the average ratio of 27 as predicted by the model. The ratio of bypass flow and Coriolis flow seems to remain more or less constant over the measurement range
- The signals of the F7 1:40 and the F7 1:99 chips behave in approximately the same ratio as the intended ratios do. As their responses have straight lines it is also implied that in this case the ratios remain constant
- The Flow-pressure graphs in the model seem to show large deviations from the graphs made from the measurement data. The inlet and outlet tubes are calculated to be not the cause of this deviation as the deviation is in the order of nanobars.

8.2 Recommendations

If the research on Coriolis mass flow sensors with bypass chips is continued then I would like to make some recommendations for research on this subject

8.2.1 Validating the model

Although the predictions made by the model seem to fit nicely I was only able to test it for one chip which is far from ideal for making conclusions on the validity of the model. Therefore the first recommendation would be to measure an F1 chip with the same chip and compare the measurement data of the F7 chips that I measured so that it can be seen if the ratios are really predicted well by the model.

The pressure range could also be increased to see if the flow ratio of the chip really declines as predicted by the model.

8.2.2 Improving the model

The Flow-pressure graphs of the model deviated a lot from the measurement data; this may be because a lot of factors weren't accounted for in the model such as temperature, the effect of bends turbulence et cetera. Therefore a good subject for a follow-up research would be a project specifically focused on adding these factors to improve the model.

8.2.3 The gas model

In this research there wasn't enough time to do measurements on the chips with gas flows. If these will be done in the future then the gas flow model that I created can be tested on its validity. This research could also be combined with the research on the inclusion of the neglected factors in the model.

8.2.4 Measurement set-up

Although I think that the second set-up was quite the improvement from the first one even now there is room for improvement as the electronics also have demolished the F7 1:24 chip when I tried to do a second measurement on that chip. Since after measurement the user usually processes the data in Matlab an improvement would be as suggested by my supervisor Jarno to drive the measurement set-up from Matlab instead of Agilent Vee as that reduces the amount of steps in the measurement-processing scheme when it is immediately processed by Matlab. Especially if you want to measure flow ratios a few lines of Matlab code are needed to get the ratio plots out. The main message in short is that when it is steered from Matlab it can more easily be customized to output what you want even while you are measuring.

Another recommendation that could be made for the measurement set-up is the suggestion to look into ways to make the phase shift measurement of the signal more reliable as the sensors, which in a feedback loop also control the chip, can make the signal oscillate a lot. This oscillation of the phase shift measurement makes it harder to get an accurate look at the data. Improving the phase shift measurement will make the analysis of the data more accurate and can save a lot of time as sometimes the measurement has to be done again because of the fact that the phase shift data is unusable.

Finally a useful thing to research is the pressure losses over the set-up as I found that the tubes were not the cause of the pressure drop. The flow controller itself would be a good place to start investigating as it has a valve, which is a component that usually has a quite large pressure loss.

8.3 Acknowledgements

First of all this report couldn’t have been made without the extensive help of my bachelor assignment committee: Remco Wiegerink, Jarno Groenesteijn and Andre de Boer for helping me get in the right direction and providing feedback. For the same reason I would also like to thank Joost Lötters for providing help especially since he wasn’t in this committee. Another person I would like to thank is Harmen Droogendijk for providing his basic maple sheet that gave me a good start ahead. Furthermore I would like to thank all others at TST for providing such a pleasant working environment and for providing a listening ear. I would like to thank my family; without their support I wouldn’t be able to make it all the way up here. At last I thank my fellow AT students who provided the well-needed distraction on my studies and made my student life that much more fun.

References

[precise]: http://mcps-precise.com/86/HOME.html

[TST]: Haneveld, J. and Lammerink, T.S.J. et al (2010) Modeling, design, fabrication and characterization of a micro Coriolis mass flow sensor. Journal of Micromechanics and Microengineering, 20 (6). p. 125001. ISSN 0960-1317

[bend]: http://www.cs.cdu.edu.au/homepages/jmitroy/eng247/sect10.pdf

[aero]: Clancy, L.J., *Aerodynamics*, Section 3.12 and 3.13

[gastemp]: Alexander J. Smits, Jean-Paul Dussauge Turbulent shear layers in supersonic flow, Birkhäuser, 2006, ISBN 0-387-26140-0 p. 46

Appendix A: Maple sheets fluid model and gas model

Fluid model maple sheet

Underneath you can find the maple model that was used in the report. A maple model already existed courtesy of Harmen Droogendijk. This model was used as a basis and the expansion on that model was added inside the maple model which I posted underneath. As you can see the results are left out this is to shorten the amount of pages of the maple model from 12 to 4. In the model two large groups of parameters are present; these can be changed depending on the situation in which you would like to use your model. Change both groups of parameters to be sure that the calculations are being carried out properly. d1 is the diameter of the Coriolis tube, whereas d2 is the diameter of the bypass tubes. For the rest of the parameters it should be no problem as those are the same as the ones used in my model.

> $restart:$

> $with(plots):$

> $eq[1] := p[ext] = p[A] + \frac{1}{2}\cdot\rho\cdot V[A]^2:$

> $p[B] := p[A] - \Delta pA:$

> $p[A] := solve(eq[1], p[A]):$

> $eq[2] := p[B] + \frac{1}{2}\cdot\rho\cdot V[A]^2 = p1a + \frac{1}{2}\cdot\rho\cdot V[1]^2:$

> $eq[3] := p[B] + \frac{1}{2}\cdot\rho\cdot V[A]^2 = p2a + \frac{1}{2}\cdot\rho\cdot V[2]^2:$

> $Q[t] := \frac{\pi\cdot d1^4\cdot\Delta p1}{128\cdot\mu\cdot l[t]}:$

$Q[b] := \frac{n\cdot\pi\cdot d2^4\cdot\Delta p2}{128\cdot\mu\cdot l[b]}:$

$Q[A] = n\cdot\frac{\pi\cdot d^4\cdot\Delta pA}{128\cdot\mu\cdot lA}:$

> $V[1] := \frac{Q[t]}{A[t]}:$

$V[2] := \frac{Q[b]}{n\cdot A[b]}:$

$V[A] := \frac{Q[A]}{n\cdot A[A]}:$

> $A[t] := \pi\cdot\left(\frac{d1}{2}\right)^2:$

$A[b] := \pi\cdot\left(\frac{d2}{2}\right)^2:$

$A[A] := \pi\cdot\left(\frac{d}{2}\right)^2:$

> $V[2]:$

> $eq[4] := 2\cdot(p[B] - p1a) + \Delta p1 + 2\cdot\Delta pA + 2\cdot(p[ext] - p[A]) = p[ext]:$

$eq[5] := 2\cdot(p[B] - p2a) + \Delta p2 + 2\cdot\Delta pA + 2\cdot(p[ext] - p[A]) = p[ext]:$

> $p1a := solve(eq[4], p1a):$

$p2a := solve(eq[5], p2a):$

> $eq[2]:$

> $\Delta p1 := \frac{128\cdot\mu\cdot l[t]}{\pi\cdot d1^4}\cdot Qcor:$

$\Delta p2 := \frac{128\cdot\mu\cdot l[b]}{n\cdot\pi\cdot d2^4}\cdot Qbyp:$

$\Delta pA := \frac{128\cdot\mu\cdot lA}{n\cdot\pi\cdot d^4}\cdot Q[A]:$

> $eq[2]:$

> $eq[3]:$

> $eq[6] := \frac{64\,\mu\,l_t\,Qcor}{\pi\,d1^4} + \frac{8\,\rho\,Qcor^2}{\pi^2\,d1^4} = \frac{64\,\mu\,l_b\,Qbyp}{n\,\pi\,d2^4} + \frac{8\,\rho\,Qbyp^2}{\pi^2\,d2^4\,n^2}:$

> $simplify(eq[6]):$

> $Q[A] := Qbyp + Qcor:$

> $eq[2]:$

> $eq[3]:$

> $\mu := 1.002\cdot10^{-3}:$

$l[t] := 17.28\cdot10^{-3}:$

$l[b] := 0.464\cdot10^{-3}:$

$n := 2:$

$d := 40\cdot10^{-6}:$

$d1 := 40\cdot10^{-6}:$

$d2 := 40\cdot10^{-6}:$

$\rho := 998:$

> $R[m] := evalf\left(\frac{l[t]\cdot n\cdot(d2)^4}{l[b]\cdot(d1)^4}\right):$

> $implicitplot(eq[6], Qbyp = 0..10^{-7}, Qcor = 0..10^{-7}, gridrefine = 6):$

> $eq[6]:$

> $eq[2]:$

> $eq[3]:$

> $Q[A] := Qbyp + Qcor:$

> $eq[1]:$

> $eq[7] := -\frac{128\,\mu\,lA\,(Qbyp + Qcor)}{n\,\pi\,d^4} + \frac{8\,\rho\,(Qbyp + Qcor)^2}{n^2\,\pi^2\,d^4} = 0:$

> $eq[2]:$

> $eq[3]:$

> $solve(eq[2], Qcor):$

> $solve(eq[3], Qbyp):$

> solve(eq[2], Qcor) :

$$> Qcor := -\frac{1}{4}\,\frac{16\,\mu\,l_t\,\pi - \sqrt{256\,\mu^2\,l_t^2\,\pi^2 + \rho\,p_{ext}\,\pi^2\,d1^4}}{\rho} :$$

> solve(eq[3], Qbyp) :

$$> Qbyp := -\frac{1}{4}\,\frac{\left(16\,\mu\,l_b\,\pi - \sqrt{256\,\mu^2\,l_b^2\,\pi^2 + \rho\,p_{ext}\,\pi^2\,d2^4}\right)n}{\rho} :$$

> eq[6] :

> solve(eq[6], Q[inlet]) :

$$> aa := \frac{1}{\rho\,(n^2-1)}\Big(\Big(4\,n\,\mu\,l_t\,\pi + n\,\rho\,Q_{inlet} + 4\,\mu\,l_b\,\pi$$

$$- \left(16\,n^2\,\mu^2\,l_t^2\,\pi^2 + 32\,n\,\mu^2\,l_t\,\pi^2\,l_b + 8\,n\,\rho\,Q_{inlet}\,\mu\,l_b\,\pi + 16\,\mu^2\,l_b^2\,\pi^2 + Q_{inlet}^2\,\rho^2 + 8\,\rho\,\mu\,l_t\,\pi\,Q_{inlet}\right)^{1/2}\Big)n\Big) :$$

$$> bb := \frac{1}{\rho\,(n^2-1)}\Big(-4\,n^2\,\mu\,l_t\,\pi - 4\,\mu\,l_b\,\pi\,n - \rho\,Q_{inlet}$$

$$+ \left(16\,n^4\,\mu^2\,l_t^2\,\pi^2 + 32\,n^3\,\mu^2\,l_t\,\pi^2\,l_b + 8\,n^2\,\mu\,l_t\,\pi\,\rho\,Q_{inlet} + 16\,\mu^2\,l_b^2\,\pi^2\,n^2 + n^2\,\rho^2\,Q_{inlet}^2 + 8\,n^3\,\rho\,Q_{inlet}\,\mu\,l_b\,\pi\right)^{1/2}\Big) :$$

$$> Rat := \frac{aa}{bb} :$$

> $\Delta p1$:

> $\mu := 1.002\cdot 10^{-3}$:
$l[t] := 17.28\cdot 10^{-3}$:
$l[b] := 0.464\cdot 10^{-3}$:
$n := 2$:
$d := 40\cdot 10^{-6}$: $d1 := 40\cdot 10^{-6}$: $d2 := 40\cdot 10^{-6}$:
$\rho := 998$:

> implicitplot(eq[6], Qbyp = 1 ..10^7, Qcor = 1 ..10^6, gridrefine = 6) :
Error, (in plots/implicitplot) invalid input: invalid range for first variable

> Rat :

> $\Delta p1$:

> loglogplot(Rat, Q[inlet] = 10^{-13} ..10^{-1}, 1 ..100) :

> Qbyp :

> Qbyp :

> plot$\left(\left[\frac{Qbyp}{Qcor}\right], p[ext] = 0 ..10^6, 0 ..100\right)$:
evalf$\left(\text{subs}\left(p[ext] = 20000, \frac{Qbyp}{Qcor}\right)\right)$:
solve$\left(\frac{Qbyp}{Qcor} = 27, p[ext]\right)$:

> plot([$3600\cdot 10^{11}\cdot$ Qbyp, $3600\cdot 10^{11}\cdot$Qcor, $1.5\cdot 9.61\cdot 10^{-15}\cdot p[ext]$], p[ext] = 0 ..10) :

Gas model maple sheet

A maple sheet for the gas model has also been made. The same instructions and story applies here as was told for the fluid model.

```
> restart:
> with(plots):
> eq[1] := p[ext] = p[A] + 1/2·ρ·V[A]^2:
> p[B] := p[A] − ΔpA:

> p[A] := solve(eq[1], p[A]):
> eq[2] := p[B] + 1/2·ρ·V[A]^2 = p1a + 1/2·ρ·V[1]^2:
> eq[3] := p[B] + 1/2·ρ·V[A]^2 = p2a + 1/2·ρ·V[2]^2:
> Q[t] := (π·d1^4·Δp1)/(128·μ·l[t]):
  Q[b] := (n·π·d2^4·Δp2)/(128·μ·l[b]):
  Q[A] = n·(π·d^4·ΔpA)/(128·μ·lA):

> V[1] := Q[t]/A[t]:
  V[2] := Q[b]/(n·A[b]):
  V[A] := Q[A]/(n·A[A]):

> A[t] := π·(d1/2)^2:
  A[b] := π·(d2/2)^2:
  A[A] := π·(d/2)^2:

> V[2]:
> eq[4] := 2·(p[B] − p1a) + Δp1 + 2·ΔpA + 2·(p[ext] − p[A]) = p[ext]:
  eq[5] := 2·(p[B] − p2a) + Δp2 + 2·ΔpA + 2·(p[ext] − p[A]) = p[ext]:
> p1a := solve(eq[4], p1a):
  p2a := solve(eq[5], p2a):
> eq[2]:
> Δp1 := (128·μ·l[t])/(π·d1^4)·Qcor:
  Δp2 := (128·μ·l[b])/(n·π·d2^4)·Qbyp:
  ΔpA := (128·μ·lA)/(n·π·d^4)·Q[A]:

> eq[2]:
> eq[3]:
> eq[6] := (64 μ l_t Qcor)/(π d1^4) + (8 ρ Qcor^2)/(π^2 d1^4) = (64 μ l_b Qbyp)/(n π d2^4) + (8 ρ Qbyp^2)/(π^2 d2^4 n^2):
> simplify(eq[6]):

> Q[A] := Qbyp + Qcor:
> eq[2]:
> eq[3]:
> μ := 0.00001870665954:
  μv := 18.27·10^(−6):
  Tv := 291.15:
  C := 120:
  l[t] := 16·10^(−3):
  l[b] := 0.8·10^(−3):
  n := 5:
  d := 40·10^(−6):
  d1 := 40·10^(−6):
  d2 := 50·10^(−6):
  ρ := (M·(p[ext] − 10^5))/(2·R·T):
  M := 32:
  R := 8.134:
  T := 300:
> R[m] := evalf((l[t]·n·(d2)^4)/(l[b]·(d1)^4)):
> implicitplot(eq[6], Qbyp = 0..10^(−7), Qcor = 0..10^(−7), gridrefine = 6):
Error, (in plots/implicitplot) invalid input: the following extra unknowns were found in the input expression: {R, p[ext]}

> eq[6]:

> eq[2]:
> eq[3]:
> Q[A] := Qbyp + Qcor:
> eq[1]:
> eq[7] := −(128 μ lA (Qbyp + Qcor))/(n π d^4) + (8 ρ (Qbyp + Qcor)^2)/(n^2 π^2 d^4) = 0:
```

$> eq[2]:$

$> eq[3]:$

$> solve(eq[2], Qcor):$

$> solve(eq[3], Qbyp):$

$>$

$> solve(eq[2], Qcor):$

$$> Qcor := -\frac{1}{4}\,\frac{16\,\mu\,l_t\,\pi - \sqrt{256\,\mu^2\,l_t^2\,\pi^2 + \rho\,p_{ext}\,\pi^2\,d1^4}}{\rho}:$$

$> solve(eq[3], Qbyp):$

$$> Qbyp := -\frac{1}{4}\,\frac{\left(16\,\mu\,l_b\,\pi - \sqrt{256\,\mu^2\,l_b^2\,\pi^2 + \rho\,p_{ext}\,\pi^2\,d2^4}\right) n}{\rho}:$$

$> eq[6]:$

$> solve(eq[6], Q[inlet]);$

$$> aa := \frac{1}{\rho\,(n^2-1)}\Big(\big(4\,n\,\mu\,l_t\,\pi + n\,\rho\,Q_{inlet} + 4\,\mu\,l_b\,\pi$$
$$-$$
$$\big(16\,n^2\,\mu^2\,l_t^2\,\pi^2 + 32\,n\,\mu^2\,l_t\,\pi^2\,l_b + 8\,n\,\rho\,Q_{inlet}\,\mu\,l_b\,\pi + 16\,\mu^2\,l_b^2\,\pi^2 + Q_{inlet}^2\,\rho^2$$
$$+ 8\,\rho\,\mu\,l_t\,\pi\,Q_{inlet}\big)^{1/2}\big)\,n\Big):$$

$$> bb := \frac{1}{\rho\,(n^2-1)}\Big(-4\,n^2\,\mu\,l_t\,\pi - 4\,\mu\,l_b\,\pi\,n - \rho\,Q_{inlet}$$
$$+ \big(16\,n^4\,\mu^2\,l_t^2\,\pi^2 + 32\,n^3\,\mu^2\,l_t\,\pi^2\,l_b + 8\,n^2\,\mu\,l_t\,\pi\,\rho\,Q_{inlet} + 16\,\mu^2\,l_b^2\,\pi^2\,n^2 + n^2\,\rho^2\,Q_{inlet}^2$$
$$+ 8\,n^3\,\rho\,Q_{inlet}\,\mu\,l_b\,\pi\big)^{1/2}\Big):$$

$$> Rat := \frac{aa}{bb}:$$

$> \Delta p1:$

$> \mu := 0.00001870665954:$
$\mu v := 18.27\cdot 10^{-6}:$
$Tv := 291.15:$
$C := 120:$
$l[t] := 16\cdot 10^{-3}:$
$l[b] := 0.8\cdot 10^{-3}:$
$n := 5:$
$d := 40\cdot 10^{-6}:$
$d1 := 20\cdot 10^{-6}:$
$d2 := 20\cdot 10^{-6}:$
$$\rho := \frac{M\cdot(p[ext] - 10^5)}{2\cdot R\cdot T} : M := 32 : R := 8.134 : T := 300:$$

$> implicitplot(eq[6], Qbyp = 10^{-8}..10^{-7}, Qcor = 0..10^{-6}, gridrefine = 6):$

Error, (in plots/implicitplot) invalid input: invalid range for first variable

$> Rat:$

$> \Delta p1:$

$$> loglogplot\left(subs\left(p[ext] = \frac{128\cdot\mu\cdot 24\cdot 10^{-3}\cdot Q[inlet]}{n\cdot\pi\cdot d^4} + 10^5, Rat\right), Q[inlet] = 10^{-7}..10^{-1}, 1..350\right):$$

$> Qbyp:$

$> Qbyp:$

$$> plot\left(\left[\frac{Qbyp}{Qcor}\right], p[ext] = 10^5..10^6, 0..500\right):$$

$$evalf\left(subs\left(p[ext] = 100000, \frac{Qbyp}{Qcor}\right)\right):$$

$> plot([Qbyp, Qcor], p[ext] = 1.1\cdot 10^5..10^6):$